Mapping of Fluidic Mixing in Microdroplets with 1 μs Time Resolution Using Fluorescence Lifetime Imaging

ARTICLE *in* ANALYTICAL CHEMISTRY · MARCH 2010

Impact Factor: 5.64 · DOI: 10.1021/ac100055g · Source: PubMed

4 AUTHORS, INCLUDING:

Xavier Casadevall i Solvas
ETH Zurich
17 PUBLICATIONS **249** CITATIONS

SEE PROFILE

Anal. Chem. **2010,** *82,* 3950–3956

Mapping of Fluidic Mixing in Microdroplets with 1 μs Time Resolution Using Fluorescence Lifetime Imaging

Xavier Casadevall i Solvas,*,† Monpichar Srisa-Art,† Andrew J. deMello,† and Joshua B. Edel†,‡

Department of Chemistry, and Institute of Biomedical Engineering, Imperial College London, South Kensington, London, SW7 2AZ, United Kingdom

Microdroplets generated in microfluidic channels hold great promise for use as substrates in high-throughput chemical and biological analysis. These water-in-oil compartments can serve as isolated reaction vessels, and since they can be generated at rates in excess of 1 kHz, thousands of assays can be carried out quickly and reproducibly. Nevertheless, sampling the large amount of information generated from these platforms still remains a significant challenge. For example, considering the high droplet generation rates and velocities, reproducibility and micrometer resolution are challenging requirements that must be fulfilled. Herein we combine confocal fluorescence lifetime imaging microscopy with a statistical implementation that permits the analysis of mixing phenomena within microdroplets with a temporal resolution of 1 μs. Importantly, such exquisite resolution is only possible as a result of the large number of droplets sampled and their high structural reproducibility.

Water droplets within a continuous oil phase generated in microfluidic channels possess a range of properties that make them attractive for use in high-throughput chemical and biological experimentation (omics, drug screening, etc.).[1−4] They are isolated and compartmentalized units, which contain only the species of interest. Indeed, in comparison to conventional single-phase microfluidic systems, localization of reagents within discrete and isolated droplets has been shown to be an effective way of enhancing reaction yields and eliminating residence time distributions. Droplets can be made to spontaneously form when laminar streams of aqueous reagents are injected into an immiscible carrier fluid, either at a T-junction or in flow-focusing geometry. Moreover, they can be generated at speeds in excess of 1 kHz while still maintaining droplet-to-droplet reproducibility in terms of content and dimensions.[2] This fact allows for both the quick repetition of a particular process under study or the multiplexing of a diversity of experiments.[3,4] Furthermore, the small sample volumes involved (typically nanoliters to femtoliters) result in reduced amounts of reagents, short diffusion lengths, reduced mixing times, and enhanced heat transfer (leading to improved temperature control).[5]

To fully benefit from the ability to generate droplets in high throughput, fast and sensitive detection techniques are required. Previous studies have reported the optical interrogation of microdroplets on millisecond time scales.[6,7] However, some important biological processes, such as protein folding or enzymatic recognition of DNA damage, proceed on time scales of a few microseconds or less.[8] Accordingly, there is significant interest and merit in reducing the time resolution of detection techniques, to accommodate the broadest range of assays possible.

Spectroscopic techniques have the ability to sample small volumes in a rapid manner. Of particular note are time domain fluorescence lifetime analysis methods that use time-correlated single-photon counting (TCSPC).[9] Such approaches have been used to determine fluorescence lifetimes at speeds of a few nanoseconds.[10] This general approach uses a pulsed excitation source and computes the delay between the arrival time of each emitted photon and a discrete excitation pulse (with a time resolution of a few picoseconds). Importantly, the molecular fluorescence lifetime is an intrinsic characteristic of an individual fluorophore that is affected only by its chemical environment. Accordingly, its measurement can be used to obtain environmental information with better resolution and precision than time-integrated fluorescence intensities, which are dependent on experimental factors (such as concentration, excitation intensity, and optical collection efficiency).[11,12] By using this technique, we recently demonstrated that fluorescence lifetime images within microdroplets could be constructed with a time resolution of 5 μs.[13] In this work, we significantly refine this imaging strategy to display the mixing patterns that develop in microdroplets as a

* To whom correspondence should be addressed. Phone: +44 (0)20 7594 5835. Fax: +44 (0)20 7594 5834. E-mail: x.casadevall-i-solvas@imperial.ac.uk.

† Department of Chemistry.

‡ Institute of Biomedical Engineering.

(1) deMello, A. J. *Nature* **2006**, *442*, 394–402.
(2) Huebner, A.; Sharma, S.; Srisa-Art, M.; Hollfelder, F.; Edel, J. B.; deMello, A. J. *Lab Chip* **2008**, *8*, 1244–1254.
(3) Song, H.; Chen, D. L.; Ismagilov, R. F. *Angew. Chem., Int. Ed.* **2006**, *45*, 7336–7356.
(4) Garstecki, P.; Fuerstman, M. J.; Stone, H. A.; Whitesides, G. M. *Lab Chip* **2006**, *6*, 437–446.
(5) Dittrich, P. S.; Manz, A. *Nat. Rev. Drug Discovery* **2006**, *5*, 210–218.
(6) Srisa-Art, M.; deMello, A. J.; Edel, J. B. *Anal. Chem.* **2007**, *79*, 6682–6689.
(7) Song, H.; Ismagilov, R. F. *J. Am. Chem. Soc.* **2003**, *125*, 14613–14619.
(8) Gruebele, M. *Annu. Rev. Phys. Chem.* **1999**, *50*, 485–516.
(9) Lakowicz, J. R. *Principles of Fluorescence Spectroscopy*, 2nd ed.; Kluwer Academic/Plenum Publishers: New York, 1999.
(10) Straub, M.; Hell, S. W. *Appl. Phys. Lett.* **1998**, *73*, 1769–1771.
(11) Robinson, T. A.; Schaerli, Y.; Wootton, R.; Hollfelder, F.; Dunsby, C.; Baldwin, G.; Neil, M.; French, P.; deMello, A. J. *Lab Chip* **2009**, *9*, 3437–3441.
(12) Edel, J. B.; Eid, J. S.; Meller, A. *J. Phys. Chem. B* **2007**, *73*, 2986–2990.
(13) Srisa-Art, M.; deMello, A. J.; Edel, J. B. *Phys. Rev. Lett.* **2008**, *101*, 014502.

10.1021/ac100055g
Published on Web 03/31/2010

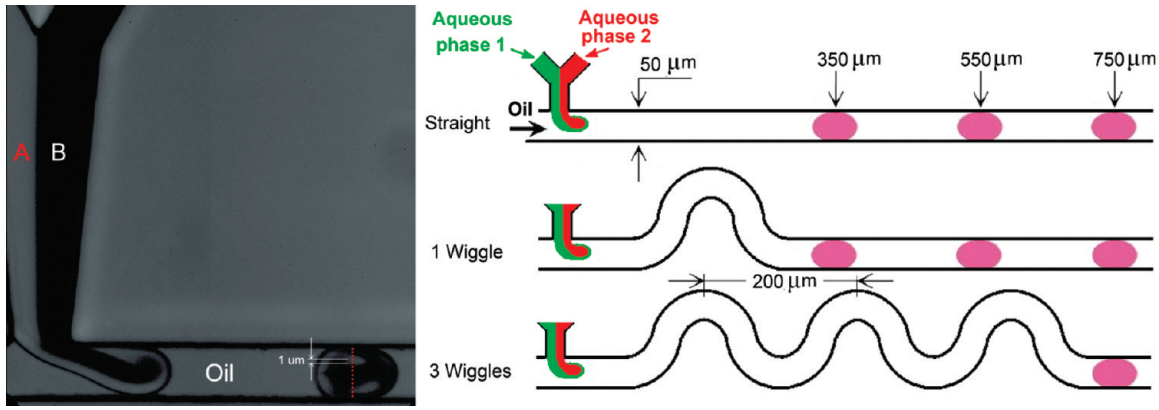

Figure 1. Water-in-oil droplets were generated from two aqueous phases (A, buffer; B, dye in buffer) flowing in parallel into a T-junction against an oil phase flow in a 50 × 50 μm^2 microchannel. The width of the channels was scanned at 1 μm intervals (red dots). Three channel configurations (straight and containing one or three wiggles) were used to map droplets under different mixing conditions.

result of convective fluxes in both straight and winding microchannels. We demonstrate that a temporal resolution along the droplet length as low as 1 μs can be achieved with acceptable error margins. These findings can have fundamental implications on the study of rapidly occurring processes in microdroplets.

EXPERIMENTAL SECTION

Experimental Setup. Microfluidic chips for droplet generation containing channels with a cross section of 50 × 50 μm^2 were fabricated using soft lithographic methods as previously described.[14] Three different kinds of channels were used in the current experiments: straight or winding and containing one or three "wiggles" downstream of the droplet formation region (Figure 1). Microdroplets were generated from two aqueous phases flowing in parallel streams at a flow rate of 1 μL/min each into a T-junction against a continuous oil flow of 6 μL/min (Figure 1). The first aqueous phase consisted of 10 μM fluorescein 5-isothiocyanate (FITC, Sigma-Aldrich) in phosphate-buffered saline (pH 7.2). The second aqueous phase contained a solution of 20 μM streptavidin−Alexa Fluor 488 conjugate (Str−AF488, Molecular Probes) in the same buffer. The oil phase was made from a 10:1 mixture of perfluorodecalin and 1H,1H,2H,2H-perfluorooctanol (both from Sigma-Aldrich).

A custom-built fluorescence confocal microscope with an automated stage (with submicrometer positioning capacity) was used to probe small volumes, of a few femtoliters, within the fluidic channels.[15] Fluorescent molecules were excited using a 485 nm pulsed diode laser (PicoQuant Gmbh, LDH-P-C-485) operating at a repetition rate of 20 MHz (50 ns pulse separation). Beam-steering mirrors were used to control the beam height as well as beam direction. A dichroic mirror (z488rdc, Chroma Technology Corp.) was used to reflect the 485 nm laser beam into the objective lens. An infinity-corrected, high numerical aperture (NA) microscope objective (Olympus 60×/1.2 NA, water immersion) brings the laser light to a tight focus within a microfluidic channel. Fluorescence emitted by the sample (within the microfluidic channel) was collected by the same high NA objective and transmitted through the same dichroic mirror. Light was then passed through an emission filter (z488lp, Chroma Technology Corp.) to remove any residual excitation light, and a plano−convex lens (+50.2 F; Newport Ltd.) focused the fluorescence onto a 75 μm pinhole. The pinhole was positioned in the confocal plane of the microscope objective. Another dichroic mirror (630dcxr, Chroma Technology Corp.) was then used to split the fluorescent signal onto two avalanche photodiodes (AQR-141, EG&G, Perkin-Elmer). Fluorescence reflected by the dichroic mirror was further filtered by an emission filter (hq540/80 m, Chroma Technology Corp.) and focused by a plano−convex lens (f = 30.0, i.d. 25.4 mm, Thorlabs) onto the first avalanche photodiode (green detector). The second avalanche photodiode (red detector) was not used in these experiments. The electronic signal from the detector was coupled to a multifunction DAQ device for data logging (PCI 6602, National Instruments), running on a Pentium PC as well as to a TimeHarp 100 time-correlated single-photon counting card (PicoQuant GmbH, Berlin, Germany) running on a separate Pentium PC. Fluorescence data were obtained using a TCSPC methodology. The raw data were deconvoluted with the instrument response function (IRF) of the detector. This was obtained using a low-concentration auramine-O solution (which has a lifetime of a few picoseconds, 2 orders of magnitude faster than the detector's response time).[16]

The optical probe volume was focused at half the height of the channels (25 μm). Beginning from the bottom side, the entire width of the channel was scanned in 1 μm intervals (illustrated with red dots in Figure 1). Measurements were performed on 6000 continuously flowing droplets for every 1 μm step. Since the probe volume was fixed and droplets were flowing across that position, a trajectory of the lifetime values along the length of the droplets could be obtained. By recording these lifetime trajectories along the entire channel width, a two-dimensional (2-D) concentration map of the droplets cross section could be constructed. These maps were built up at various locations downstream from the droplet forming region (350, 550, and 750 μm) for all channel designs (note that for the "three-wiggles" design only the 750 μm position was mapped). Mapping of the droplets was performed in order to visualize the effect of "wiggles" on mixing efficiency. An illustration of the process and the devices used is presented in Figure 1.

(14) McDonald, J. C.; Whitesides, G. M. *Acc. Chem. Res.* **2002**, *35*, 491–499.
(15) Srisa-Art, M.; Dyson, E. C.; deMello, A. J.; Edel, J. B. *Anal. Chem.* **2008**, *80*, 7063–7067.
(16) Edel, J. B.; deMello, A. J. *Appl. Phys. Lett.* **2007**, *90*, 053904.

Theory. The fluorescence decay of a single molecular species should ideally follow a monoexponential decay function. However, in a mixture containing two (noninteracting) fluorescent species the decay will take on a biexponential form as is shown in eq 1.

$$I(t) = \alpha_1 e^{-t/\tau_1} + \alpha_2 e^{-t/\tau_2} \quad (1)$$

The individual lifetimes are defined as τ_1 and τ_2, and the amplitude of each component is defined as α_1 and α_2, respectively. The average lifetime can then be defined as follows:

$$\bar{\tau} = \tau_1\beta_1 + \tau_2\beta_2 \quad (2)$$

Here β_1 and β_2 are the fraction of each component and are defined as follows:

$$\beta_1 = \frac{\alpha_1}{\alpha_1 + \alpha_2}, \quad \beta_2 = \frac{\alpha_2}{\alpha_1 + \alpha_2} \quad (3)$$

Importantly for a two-component system the average lifetime, $\bar{\tau}$, and fractional amplitudes, β_1 and β_2, are therefore directly proportional to the degree of mixing within the droplet.

A numerical algorithm was implemented to extract the lifetime and intensity values[12] for each experiment. Initially the algorithm differentiates signal bursts (associated with droplets) from the noise background of the oil phase and establishes the duration of each burst. A maximum likelihood estimator (MLE) algorithm is used to evaluate the fluorescence lifetime, as defined by eq 4:

$$\gamma_j = \sum_{l}^{k} n_i \log\left(\frac{n_i}{N p_i(j)}\right) \quad (4)$$

where n_i is the number of photon counts in channel i, k is the number of channels (or bins) for each fluorescence decay, and $p_i(j)$ is the probability that a group of photons will fall in channel i if the particles have a lifetime j.[17] $N = \sum_1^k n_i$ is the total number of photons in a given decay. For a fluorophore following an exponential decay convolved with the IRF, eq 4 can be shown to have the following form:[12]

$$\frac{N}{1 - e^{-\omega/r}} - \frac{N}{e^{k\omega/\bar{\tau}} - 1} = \sum_{i=1}^{k} i n_i \left(\frac{i - \sum_{j=1}^{i} j r_j e^{j\omega/\bar{\tau}}}{\sum_{j=1}^{i} r_j e^{j\omega/\bar{\tau}}} \right) \quad (5)$$

The IRF contribution to the decay corresponds to r_j in each bin j, recorded with a time resolution ω. The fluorescence lifetime, $\bar{\tau}$, can then be extracted by using a minimization routine such as a Levenberg−Marquardt algorithm. It is important to note that the MLE used in this method only determines the average lifetime of the mixture and not the individual components.

Three parameters directly affect the standard error of the measured lifetime using eq 5. They are as follows: (1) the total number of photons, N, used in a given decay, (2) the time resolution of the experiment (which is directly proportional to the spatial resolution), ω, and (3) the number of bins, k, used in each measurement. This also depends directly on the number of droplets used in the computation. For example, using a 5 μs time resolution and 20 photons, the standard error with a 95% confidence is 44%.[13] Averaging the results among the droplets sampled during the experiment reduces the error by the square root of the number of photon counts. Trying to reduce the time resolution, though, has the opposite effect, since it increases the number of channels, therefore reducing the effective number of photon counts per channel. Hence, to maintain the data within the limits of an acceptable error, if the time resolution is sought to be reduced, it is necessary to increase the number of analyzed droplets proportionally (i.e., the error for 600 droplets and 10 μs time resolution is 3%, the same as for 6000 droplets and 1 μs time resolution).

RESULTS AND DISCUSSION

The TCSPC experiments provide a measure of the degree of mixing between the two species present. Initial experiments revealed that the fluorescence lifetimes for pure FITC and Str−AF488 were 4.1 and 3.1 ns, respectively. Mixtures of these two components revealed lifetimes in between these limits as described by eq 2. As stated this provides a linear relationship between lifetime and composition. Since the starting concentrations of FITC and Str−AF488 are 10 and 20 μM, respectively, a perfectly mixed solution (containing a FITC to Str−AF488 molar ratio of 1:2) has a lifetime of ~3.4 ns.

Figure 2 shows the lifetime and intensity trajectories along the length of the droplets scanned at a particular width (35 μm above the lower side of the channel). These experiments were carried out in a channel containing one wiggle, and trajectories were obtained at a position 550 μm downstream from the droplet formation T-junction. These trajectories were formed as follows. Individual droplets were identified using a Matlab custom-built algorithm that could discriminate between fluorescent signal and background. All photons were recorded with a macroscopic time resolution of 50 ns (relative to the droplet's initial fluorescence burst) and a microscopic time resolution of 37 ps. The macroscopic time resolution was used for determining the relative position within the droplets while the microscopic time resolution was used for determining the fluorescent lifetime. To determine the fluorescent lifetime, the raw data was binned into groups of 20 sequential photons. Each group of 20 photons was used to calculate a single lifetime using the MLE algorithm. Furthermore, each group of 20 photons was given a new macroscopic time based on the average of the 20 photons. The process allowed for both lifetime and intensity trajectories to be obtained for a single droplet at a single detection point. This procedure was carried out for every droplet in the experiment. To reduce the error of this approach, these trajectories could then be averaged among all the droplets probed as there is little change when comparing the droplet-to-droplet composition. To do so, the individual droplet trajectories were rebinned with a well-defined time resolution (either 10 or 1 μs). Once this was done, the individual droplet trajectories could be averaged. The droplet averaged lifetime and intensity trajectories are shown in Figure 2a−c.

Each subfigure illustrates the effect of changing the number of droplets used for the calculation and reducing the time

(17) Kollner, M.; Wolfrum, J. *Chem. Phys. Lett.* **1992**, *200*, 199–204.

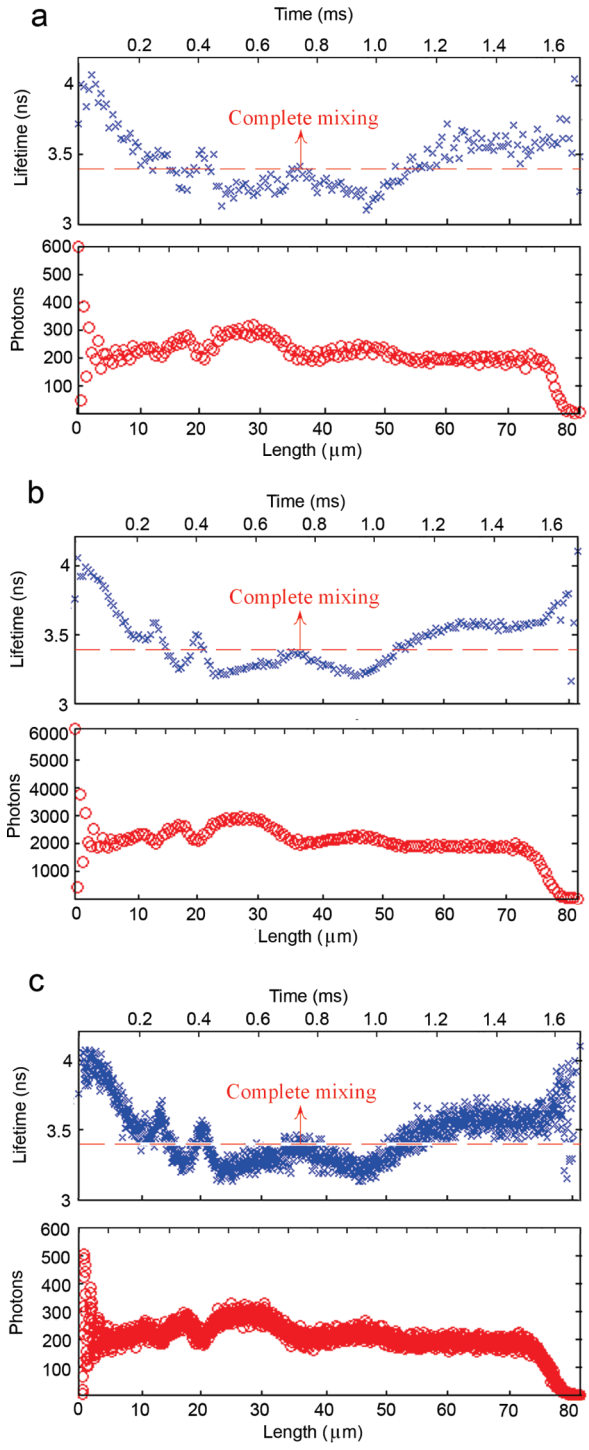

Figure 2. Lifetime and intensity trajectories (values along the droplet length) for droplets generated in a one-wiggled channel, 550 μm away from the T-junction and at width position of 35 μm: (a) average for 600 droplets and 10 μs time resolution; (b) average for 6000 droplets and 10 μs time resolution; (c) average for 6000 droplets and 1 μs time resolution. Standard errors are 3%, 1%, and 3%, respectively, at a 95% confidence interval. Dotted red lines represent perfect mixing at 3.4 ns.

resolution on the lifetime and intensity trajectories obtained. The number of droplets and the time resolution used in each calculation was 600 droplets and 10 μs (for Figure 2a), 6000 droplets and 10 μs (for Figure 2b), and 6000 droplets and 1 μs (for Figure 2c). Using counting statistics, the relative error at 95% confidence interval can be calculated as follows:

$$\%\mathrm{err}_B = \frac{2\sigma}{N} = \frac{2\sqrt{N}}{N} = \frac{2\sqrt{20B}}{20B} = \frac{2\sqrt{20}}{20}\frac{\sqrt{B}}{B} = \frac{2\%\mathrm{err}_{20}}{\sqrt{B}} \quad (6)$$

where N is the total number of photons and B is the number of averaged lifetimes for a single point (as in Figure 2). Err_{20} is the relative error for the MLE lifetime estimation using 20 photons (44.72%). The relative error is 1% for Figure 2b and 3% for Figure 2, parts a and c. This error is a direct result of the number of photons used per lifetime estimation and hence the total number of droplets being used for determining each averaged lifetime.

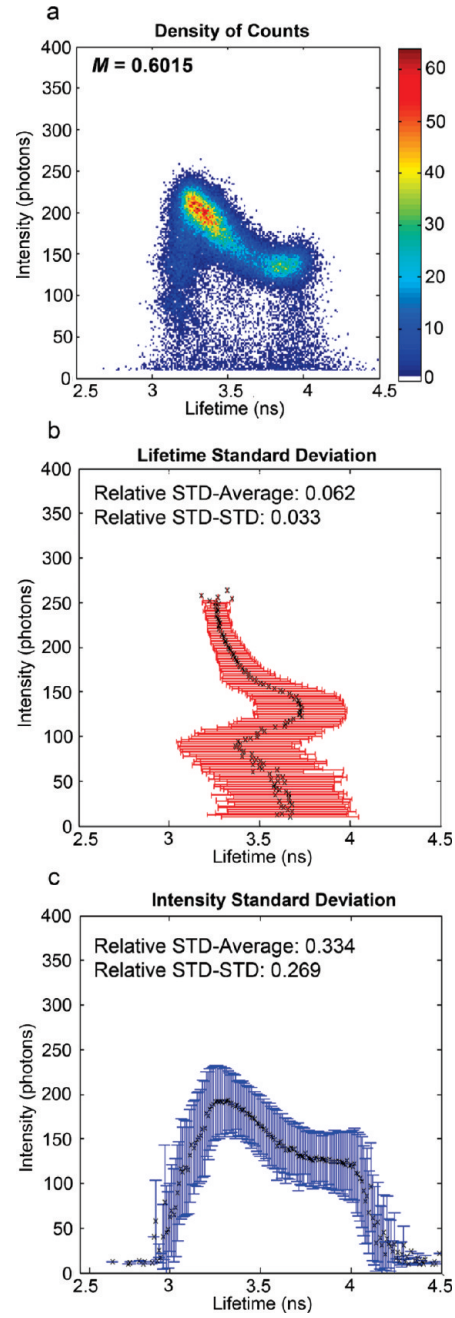

Figure 3. Results of the experiments carried out along the whole width of 6000 droplets in a straight microchannel, 350 μm downstream from the T-junction and with 1 μs time resolution: (a) lifetime vs intensity plot, including the value of the mixing coefficient M; (b) lifetime distribution (mean and standard deviation) for fixed intensities at intervals of 10 photons; (c) intensity distribution (mean and standard deviation) for fixed lifetimes at intervals of 0.01 ns.

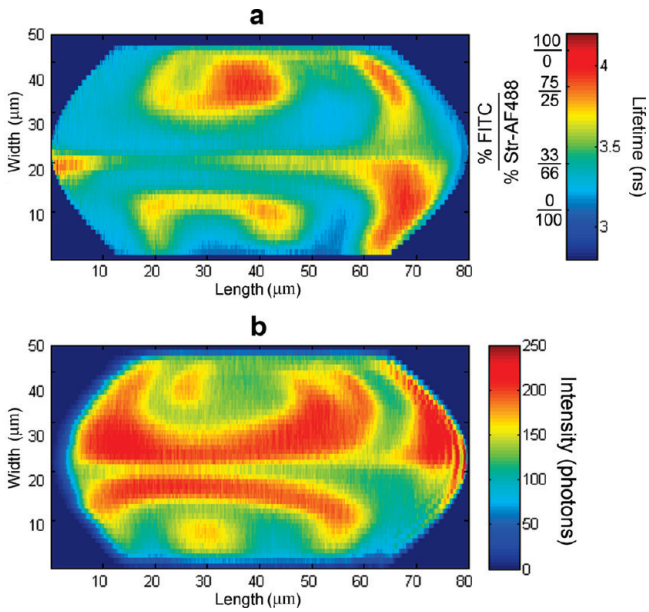

Figure 4. Two-dimensional maps of droplets in a straight channel 550 μm away from the T-junction with 1 μs time resolution. Plots are constructed using (a) lifetime and (b) intensity data to fit the shape of the imaged droplets. Plot a includes a scale bar with the composition of FITC and Str−AF488, with a ratio of 1:2 (33%/66%) representing a perfectly mixed solution. The intensity plot, b, is clearly seen to decay at the bottom and left edges, which renders the conversion into compositions unfeasible.

The plots in Figure 2 are built using length units to illustrate the droplet's geometry. The width is built with 1 μm pixel resolution (which is the distance between experiments along the width of the channel), and the length is linked to the time resolution. Approximately 80 μm in length correlated to 1.7 ms. Hence, a time resolution of 1 μs corresponds to a pixel length resolution of ~50 nm (not to be mistaken for the microscope's spatial resolution, which for our system is approximately 220 nm).

The fluorescence lifetime, as a measure of chemical composition, is a more suitable parameter than intensity alone. This statement is supported by inspection of Figure 3, which presents data comprising the scans of the whole width of 6000 droplets in a straight channel at a 350 μm distance from the T-junction. Figure 3a shows a plot of lifetime versus intensity data that was constructed by rebinning the lifetime and intensity data in bins of 0.01 ns and 10 photon counts, respectively. A large spread of both sets of data is observed; however, the lifetime data displays a higher degree of compactness. In Figure 3b the mean and the standard deviation of the lifetime values are presented for fixed intensity values at intervals of 2 photons. In Figure 3c, the fluorescence lifetime was fixed at 0.01 s intervals and the mean and standard deviation of the intensity is presented. By normalizing the standard deviations over their mean, the average of the relative standard deviation can be obtained. It can be seen that, for the fluorescence lifetime, this value (0.06) is about 2 orders of magnitude smaller than for the intensity (0.33). In addition to its lower spread, the fluorescence lifetime is characteristic of each fluorophore and independent of factors such as concentration. In fact, intensity not only depends on concentration but also on the

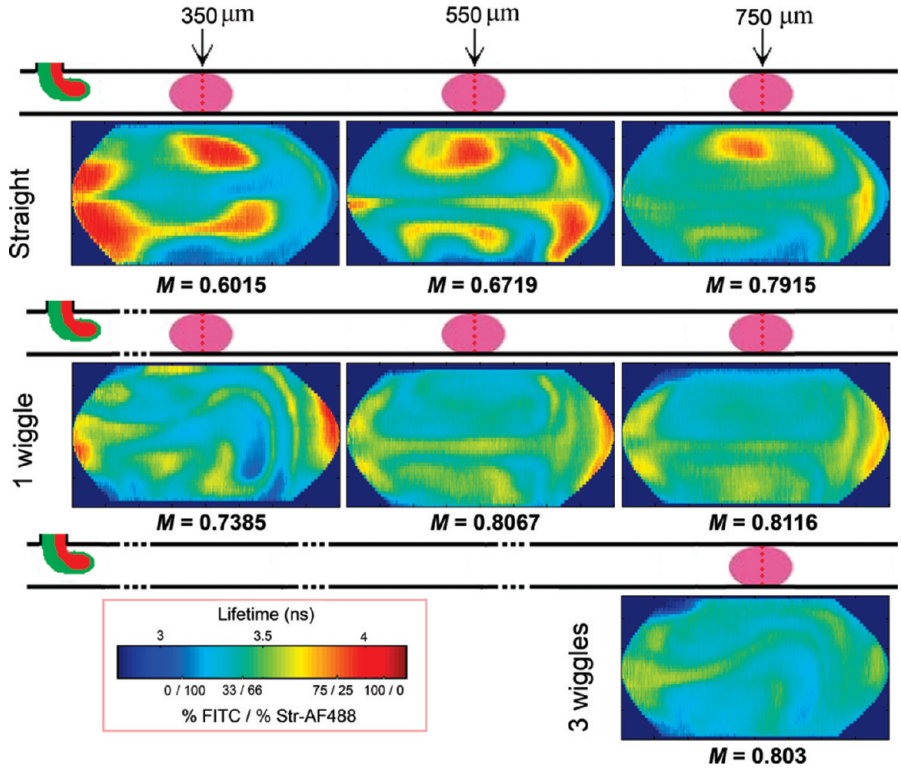

Figure 5. Fluorescence lifetime maps of droplets generated in three different channels, containing either zero (straight), one, or three wiggles. The images were obtained at different positions downstream from the T-junction for each channel (350, 550, and 750 μm for zero- and one-wiggle channels and 750 μm for the three-wiggles channel) for comparison. Complete mixing is reached at 3.4 ns, which represents a ratio of 1:2 (33%/66%) of FITC/Str−AF488. Mixing is achieved by means of diffusion (which increases with residence time) and convective flux within the droplet caused by the shear forces at the water−oil interface. As the mixing factors, *M*, indicate, the presence of wiggles increases the complexity of the internal flows enhancing mixing.

peculiarities of the system under study. For instance, in droplets, the intensity values at the edges will vary substantially. At the tail of the droplet (Figure 3a for lifetimes around 4 ns and Figure 2 for droplet length values from 0 to 5 μm), intensity values have a large dispersion, but the fluorescence lifetime is quite stable. At the head of the droplet, for lengths between 75 and 80 μm in Figure 2, intensity decays quickly to zero, invalidating its use as a concentration estimator since it can no longer be associated with the concentration of a particular fluorophore; hence, lifetime is the only reliable concentration estimator in this scenario. These edge effects may arise from the spherical shape of the droplets (which may permit part of the probe volume to sit on the outside of the actual droplet at the boundaries) and of droplet size variability (probing shorter and longer droplets would introduce a degree of measurement variability at the edges). For all these reasons, the fluorescence lifetime is a more reliable measurement in the evaluation of concentration in droplets.

To obtain a map of the concentration profiles inside droplets the following procedure was carried out. Initially droplets were generated under the same experimental conditions used for the fluorescence lifetime measurements and pictures were taken using a high-speed CCD camera. Subsequently, the lifetime and intensity data obtained with the TCSPC method were rebinned accounting for the shape of the imaged droplet so that the trajectories obtained at each width would match the actual droplet size. Figure 4 illustrates an example of mapping droplets using either lifetime or intensity data. Here it is again demonstrated that intensity is a less reliable parameter when mapping droplet composition, since at the edge (due to the lower number of photon counts recorded) it is not possible to discern the concentration of the species present.

Following this procedure, droplets for all channels and selected positions were mapped, and the results are shown in Figure 5. Mixing in microdroplets is achieved due to two main mass transport effects: diffusion and convection. The first is based on concentration gradients and the second on the internal flows that are generated within droplets due to the shear forces exerted at the water−oil interface. The presence of wiggles in the channels induces more complex internal flows that generate chaotic advection (stretching and folding of fluid elements leading to improved mixing).[18]

In the straight channel the internal flow is symmetrical with the channel direction. Two symmetrical flows are generated in the top and bottom halves of the droplet that do not interconnect: a divisive line is clearly observed at the center of the droplet, whereas two symmetrical recirculation vortices form in the top and bottom halves (Figure 5, straight and one-wiggle channels at 550 and 750 μm). For winding channels, however, it can be clearly observed that this symmetry is broken, and flows connecting the top and bottom halves of the droplet are generated (Figure 5, one wiggle at 350 μm and three wiggles at 750 μm). This is precisely the effect responsible for the enhancement of mixing in these configurations. The further down the channel the droplets are mapped, the longer the residence time and the more thorough the mixing (as noted, complete mixing is observed at a lifetime of 3.4 ns, mapped in a green color in Figure 5). Importantly, the concentration distributions observed using our approach are in

(18) Aref, H. *J. Fluid Mech.* **1984**, *143*, 1–21.

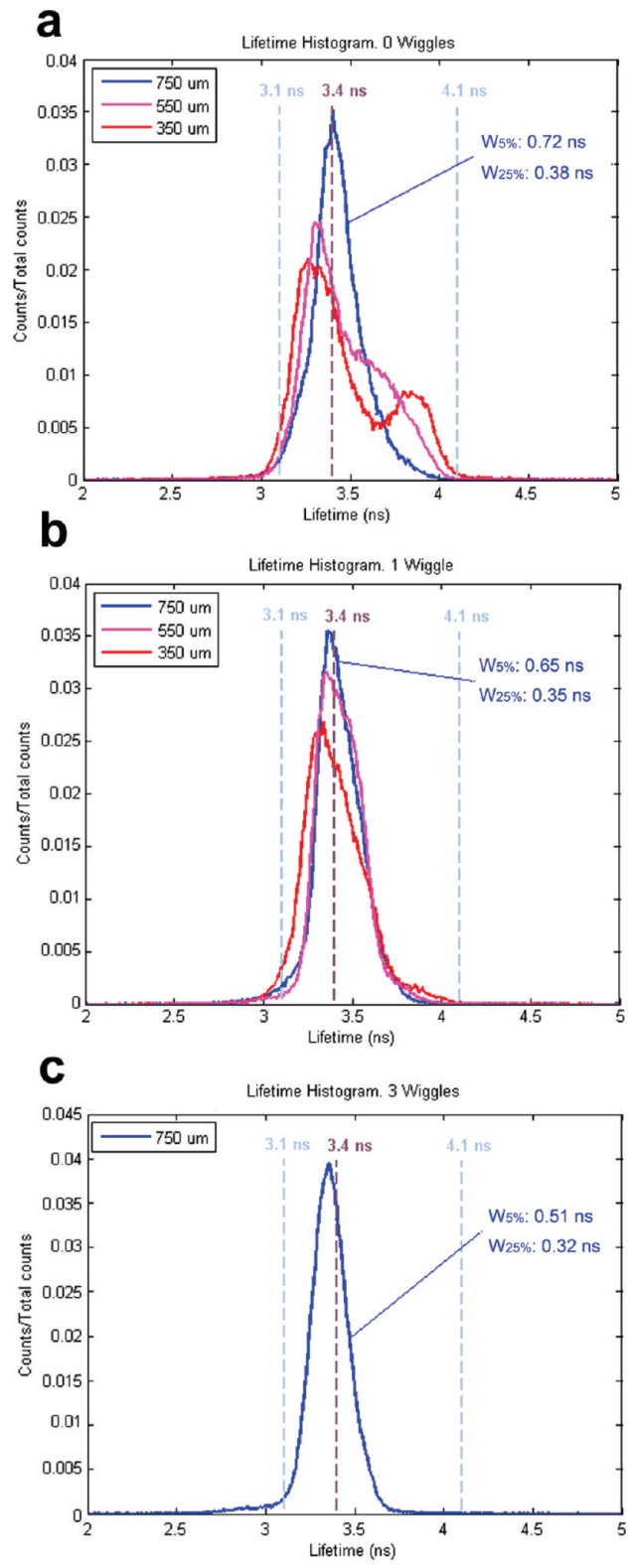

Figure 6. Lifetime histogram distributions of the 2-D maps (at intervals of 0.01 ns) are presented for three channel configurations: (a) straight, (b) one "wiggle", and (c) three "wiggles". Lower degrees of mixing result in two distributions with maxima at 3.1 and 4.1 ns, respectively (350 μm). Higher degrees of mixing result in a single distribution centered at 3.4 ns (750 μm). The widths of the histograms at 5% and 25% of the peak height ($W_{5\%}$ and $W_{25\%}$) are also illustrated as they give complementary information when compared the *M* coefficient.

agreement with previous flow dynamics studies using Micro Particle Imaging Velocimetry (μ-PIV) and numerical simulations in microdroplets in both straight and winding channels,[19] but with a time resolution that is reduced by 3 orders of magnitude.

In our experiments it is readily appreciated that the presence of these wiggles has an immediate effect on concentration distribution, and the contribution of this effect on mixing efficiency can be precisely quantified using the lifetime data obtained to construct the maps. For this purpose a mixing coefficient, M, was defined as follows. For a perfectly mixed droplet, all photon counts would fall on a straight line with a lifetime value of 3.4 ns. For a perfectly separated mixture two straight lines would be obtained at 3.1 and 4.1 ns, respectively. Therefore, the total amount of mixing could be estimated by comparing the lifetime obtained from that of the perfectly mixed state. Experimentally this was calculated by grouping all data points into two groups, one containing the total amount of points on the right-hand side (RHS) of 3.4 ns and the other containing the total number of points on the left-hand side (LHS). With this, M could be defined using eq 7, which takes on a value of 0 for a perfectly unmixed solution (all points have a lifetime of either 3.1 or 4.1 ns, or $D_{mix} = D_{no\ mix}$) and 1 for a perfectly mixed solution (all points have a lifetime of 3.4 ns, or $D_{mix} = 0$).

$$M = \frac{D_{no\ mix} - D_{mix}}{D_{no\ mix}} \tag{7}$$

All plots in Figure 5 are accompanied by their M coefficient estimation. It can be seen that the immediate effect after one wiggle, when compared to a straight channel, significantly increases mixing (Figure 5 at 350 μm). But at longer lengths, as for all droplets at 750 μm, M actually takes comparable values. To further understand the mixing efficiency, lifetime histograms of the maps were plotted as shown in Figure 6. The width of each distribution in Figure 6 was calculated at 5% and 25% of the peak maxima. The narrower the distribution, the better the mixing efficiency. As illustrated in Figure 6, for all histograms at 750 μm, a narrower distribution was found in the data sets corresponding to better mixing. The histograms also nicely demonstrate that the mixing efficiency improved with the number of "wiggles" used. The height of the peaks is also a good indicator of the width of the distribution as the higher the value at 3.4 ns the greater the mixing. This estimation of mixing complements the M coefficient since small variations on the actual lifetime value of a perfectly mixed sample can alter the calculation of M, but they will not affect the data from the histograms. This can be readily appreciated for the channel with three "wiggles", where the histogram is not perfectly centered at 3.4 ns. This can be due to a slight change in chemical composition of the sample resulting in a shift from 3.4 ns for a perfectly mixed sample. This is likely to be the reason why the M coefficient for a "three-wiggles" channel was smaller than that for a "one-wiggle" channel.

As a final consideration it is worth discussing these results in the frame of the possible applications of this technique. In this study droplets were generated at an approximate frequency of 200 Hz. Considering their dimensions (80 μm in length) and the duration of the droplet bursts (of about 1.7 ms), the speed of the droplets was approximately 50 μm/ms. Therefore, it took about 15 ms for a droplet to cover a distance of 750 μm. As presented above, the degree of mixing after only three wiggles and 15 ms was about 80%. Taking into account the fact that droplets can be generated at faster rates mixing would be accelerated. Decreasing the size of the channels would also contribute to the mixing efficiency.

CONCLUSIONS

A method for imaging lifetime fluorescence events in microdroplets with a time resolution of 1 μs with a 3% standard error at a 95% confidence interval has been developed and presented. We have used this technology to visualize the mixing of two fluorescent dye solutions within different configurations of microchannels containing zero (straight), one, or three wiggles. The effects of such wiggles on mixing efficiency can be readily observed and quantified with this technique.

ACKNOWLEDGMENT

This work was supported by the RCUK Basic Technology Programme and EPSRC.

Received for review January 8, 2010. Accepted March 12, 2010.

AC100055G

(19) Malsch, D.; Kielpinski, M.; Merthan, R.; Albert, J.; Mayer, G.; Köhler, J. M.; Süsse, H.; Stahl, M.; Henkel, T. *Chem. Eng. J.* **2008**, *135-S1*, S166–S172.